Braiding of Composite Tubes using Pre-Impregnated Carbon Fibre/Thermoplastic Tapes for Airships

E. Frandsen[1*], and L. Laberge Lebel[1]

[1] Advanced Composite and Fibers Structures Laboratory (ACFSlab), High Performance Polymer and Composite Systems (CREPEC), Polytechnique Montreal, Montreal, Canada,

* *Corresponding author (evans.frandsen@polymtl.ca)*

Keywords: *braid; prepreg tape; thermoplastic; carbon fibre; PEKK;*

Abstract

Composite tubular structures offer high strength-to-weight ratios, making them ideal for advanced air mobility vehicles. Multi-layer braided designs enable continuous structures capable of withstanding complex loads. Thermoplastic matrices further enhance versatility by allowing remelting and welding, facilitating the fabrication of larger, more intricate truss structures. This work examines the relationship between mandrel diameter, braiding, and axial yarns in composite tubes made with carbon fibre preimpregnated polyetherketoneketone (PEKK) yarns. Using triaxial and biaxial braid unit cells; cover factor, minimum braid diameter, and maximum axial yarn width were derived. Preliminary regular and diamond braids of varying sizes were then fabricated based on these geometric predictions. Experimental results aligned well with geometric unit cell calculations for cover factor, minimum diameter, and axial yarn relationships. However, braid angle control proved challenging due to the high stiffness of the pre-impregnated yarns, causing them to default to relatively low braid angles. Future work will focus on improving tension management, upgrading carriers, and exploring different braider setups to enhance braid quality.

1. Introduction and Background

Advanced air mobility (AAM) vehicles are a focus of increased research due to their versatility. Many countries including Canada have been funding projects involving AAM vehicles for future development [1]. Airships for example can carry large payloads to hard-to-reach northern communities in Canada. Helium based airships are planned for this purpose. Due to the switch from hydrogen to helium, improved technology is required to lift similar or greater loads to what has been done in the past. For this reason, composite materials are an attractive solution due to their high strength-to-weight ratio, reducing structural weight while retaining the necessary mechanical properties.

The type of matrix used in composites affects everything from mechanical properties to the particulars of fabrication and consolidation. Historically, epoxies and other thermosets have often been used due to their desirable mechanical properties and chemical resistance [2]. Recent research has been starting to focus on the use of thermoplastic matrix composites due to their recyclability and ability to be remelted after initial consolidation [3-5]. This allows the welding of thermoplastic based structures [6, 7]. Thermoplastic composites come in the pre-consolidation state of separate fibres that can be commingled or co-wound with the reinforcing fibres or pre-impregnated with the reinforcing fibres (prepregs) [8, 9].

Composites combine two or more physically bonded materials with tailorable properties. One common form involves impregnating textile fibres with a polymer matrix, either before, during, or after structuring the textile. Examples of composite structures include filament winding, weaving, and braiding. Braiding involves the continuous interlacement of yarns along an axis, similar to weaving but with yarns interlaced along a length rather than forming a sheet [10]. Braiding can be adjusted to construct preforms and structures of various geometries. Figure 1 presents a schematic of a maypole braider, which is a machine commonly used to construct braided preforms. The preform is constructed at the centre of a circular pattern of horngears pushing carriers along a sinusoidal track. The green and orange carriers in Figure 1 go in opposite directions around the preform. The preform is often braided onto a mandrel of a desired shape and size. Adding a matrix to the braid makes a thin-walled composite structure, a tubular braided composite (TBC). Figure 2 shows common braided preform patterns. These are biaxial braid patterns, meaning two interlacing yarn axes around the mandrel. Biaxial patterns include 2 over 2 (regular, Figure 2(a)) and 1 over 1 (diamond, Figure 2 (b)). Biaxial braids can be broken down into the smallest repeatable unit cell of the braid (Figure 2 (c)). The type of braid fabricated in a maypole braider is controlled by the ratio of carriers to horngears. Using twice the number of carriers as horngears produces regular braids. Using the same number of carriers as horngears produces diamond braids. Other permutations are possible, which will produce a regular or diamond braid with a number of carriers that is some fraction of the total number of horngears. Axial yarns can also be added along the axis of the braid, making triaxial braids.

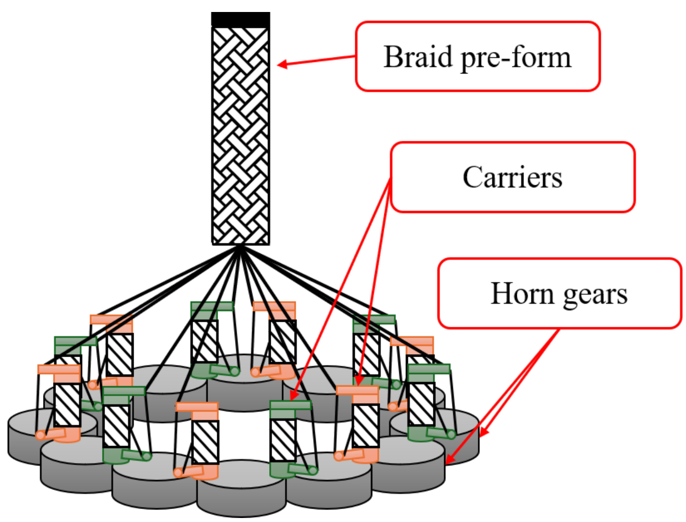

Figure 1. Schematic of a vertical maypole braiding machine

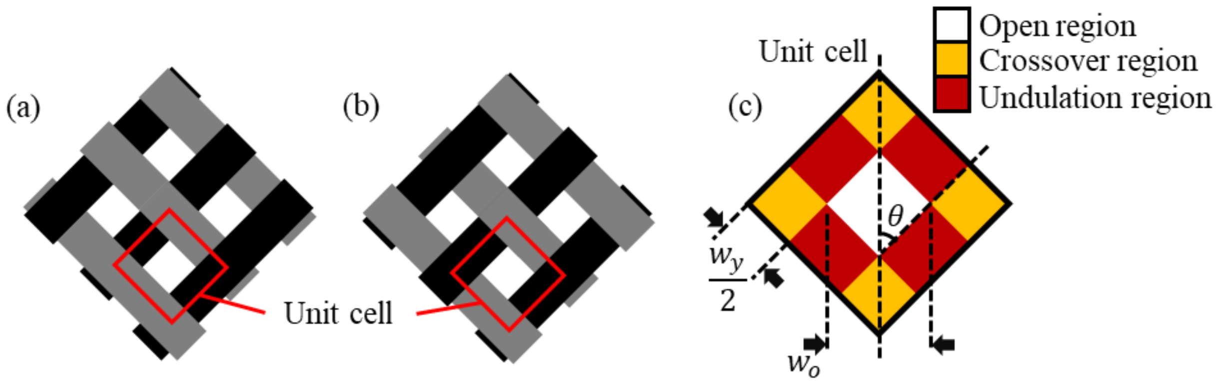

Figure 2. Examples of (a) 2 over 2 regular and (b) 1 over 1 diamond braiding structure patterns with (c) the unit cell showing braid angle, yarn width and open region width

The braiding of prepreg materials has the same basic geometry and patterns as typical textile braiding. Key differences being an increase in stiffness of the yarn and a change from a lenticular shape that conforms to the available space with loose yarns to a predetermined rectangular profile with prepreg yarns [11]. Previous work has been done to construct TBCs with prepreg tape yarns. Garthaus designed carriers for prepreg braids and did work on their consolidation for forming functional structural pieces [12]. Wurfel et al. advanced this work by using overmolding technology to fabricate car drive shafts using injection moulding [13]. Mischorr et al. used the braiding of Garthaus with a curved mandrel and bladder assisted and rotational moulding [9]. Their work demonstrated one of the primary issues of braiding with prepreg yarns in a scaling effect caused by the helical path of a braiding yarn and the prepregs higher cross-sectional stiffness. Li et al. have demonstrated the pultrusion of carbon fibre (CF)/Polyetheretherketone (PEEK) TBCs and their subsequent welding to form a truss for on-orbit fabrication [14]. None of the research discussed has demonstrated the particulars of prepreg tape braid parameters and how they differ from regular loose yarn braids.

Potluri et al. worked to define the geometric modelling of braided composites [15]. Some major products of their work are the definition of a unit cell with a width, w_{uc}, of

$$w_{uc} = \frac{2\pi D}{N_c} \tag{1}$$

where D is the braiding mandrel radius and N_c is the number of carriers. The unit cell was then used in finding the braid cover factor, CF,

$$CF = 1 - \left(1 - \frac{w_y N_c}{2\pi D cos(\theta)}\right)^2 \tag{2}$$

where w_y is the yarn width, and θ is the braid angle. When $CF = 1$, the braid fully covers the mandrel.

This work aims to geometrically model and experimentally validate the relationship between mandrel diameter and braiding/axial yarn dimensions and how they affect CF in TBCs with prepreg tape yarns. The unit cell model is adapted to model braids with prepreg tapes. Several braids were made and compared with the braid properties given by the unit cell model.

2. Geometric Model

The geometric modelling by Potluri et al. is used as a starting point for the geometric modelling of braids with prepreg tapes herein. The advantage of modelling braids with tapes is that their cross-section geometry is independent from the chosen braiding parameters. There is no tape width variation due to inter-tape contact in the braid since the fibres in the tape are consolidated. This makes the geometry easier to predict for a given θ. In the geometric design of a braid with prepreg tapes, the w_y is standardized, θ is chosen for a desired mechanical application and N_c is often given by the braider. We pose here methods for finding the desired or necessary mandrel diameter given these parameters.

2.1. Biaxial Braid

Generally, the relationship between a mandrel diameter and braiding yarn width in a TBC can be defined by,

$$D = \frac{N_c}{2\pi}\left(\frac{w_y}{\cos\theta} + w_o\right) \tag{3}$$

where w_o is the width of the open region in the braid unit cell (Figure 2 (c)). The relationship is valid whether the braid is regular or diamond. The equation can similarly be used to find the minimum mandrel diameter for a given w_y by letting w_o approach zero.

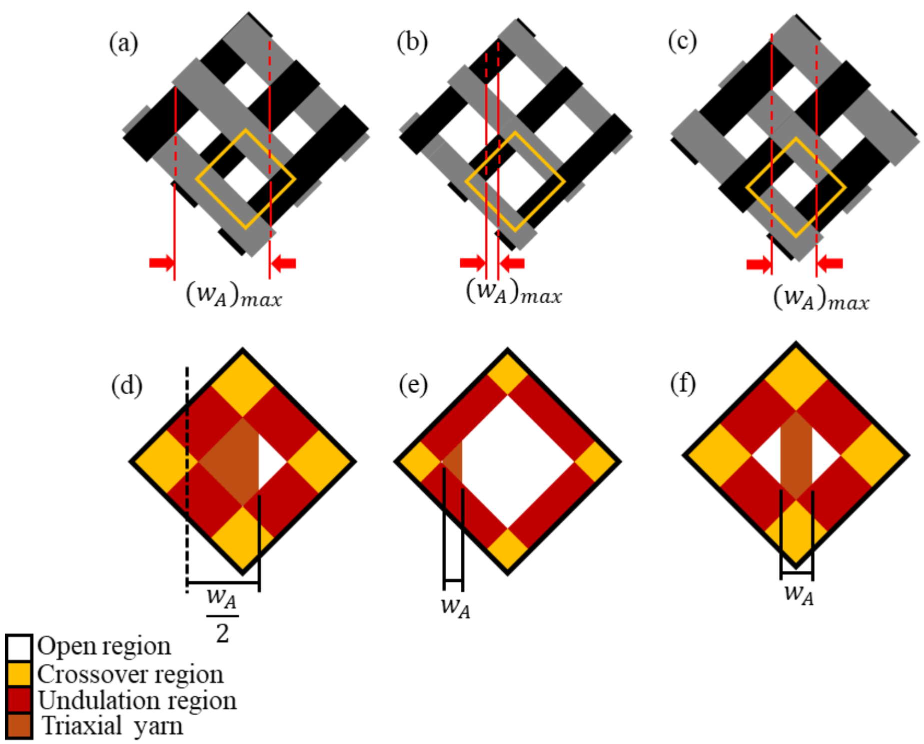

Figure 3. Maximum axial yarn width in a (a) regular braid axial yarn, (b) special case regular braid with a middle axial yarn, (c) diamond braid axial yarn, where the dotted red line shows the outline where a triaxial yarn would be going under a yarn and the solid red line shows the axial yarn outline. Below each maximum axial yarn schematic are the corresponding outlined unit cells, showing how the axial yarn affects the unit cell for the (d) regular braid axial yarn, (e) special case regular braid with a middle axial yarn, (f) diamond braid axial yarn

2.2. Regular Triaxial Braid

Figure 3 (a,b,c) presents regular and diamond braid patterns with outlines of maximum axial yarn widths, $(w_A)_{max}$, in red. The maximum axial yarn width lines are dashed when going under a yarn and solid when going on top relative to the perspective of the reader. Figure 3 (a) shows a regular braid with axial yarn of $(w_A)_{max}$ centred between two staggered crossover regions. Figure 3 (b) shows a special case regular triaxial braid where the axial yarn has an inversed over under pattern, $(w_A)_{max}$ is limited by adjacent staggered cross over regions. Figure 3 (c) shows a diamond triaxial braid where $(w_A)_{max}$ is constrained by adjacent crossover regions along the braid circumference. Subfigures (d,e,f) presents the corresponding unit cell outlined in orange in (a,b,c). The unit cells present non maximum axial yarn coverage for the purpose of visualizing how the yarn fits in the cell, with the axial yarn width, w_A, shown. Figure 3 (d) shows the regular triaxial unit cell with the axial yarn centred at the quarter point which corresponds to the halfway point between two staggered unit cells. Figure 3 (e) shows the inverse regular triaxial unit cell where the axial yarn is centred in the same manner to Figure 3 (d). Figure 3 (c) shows a diamond triaxial unit cell where the axial yarn is centred with the crossover regions at the centre of the unit cell.

For a regular braid, the axial yarn sits in the crossover region and will not affect its diameter until it is

$$\frac{w_y}{2\cos\theta} + 1.5w_o \geq w_A \tag{4}$$

which is difficult to implement and generally impractical since axial yarns require through holes that are geometrically limited by the size of horngears and their hollow rotation axes. An inverse middle yarn is one exception to this that is further discussed in the next section. The maximum axial yarn width for a regular braid is the space between two staggered open regions, comprising one entire crossover region (Figure 3 (a)). The cover factor for the regular triaxial braid ($CF_{3ax,reg}$) is derived from the Potluri et al. unit cell (Equation (1)) with added area covered by the axial yarn (see Figure 3 (d)), with

$$CF_{3ax,reg} = \begin{cases} 1 + \left(\frac{1}{2} + \frac{N_c}{2\pi D\cos\theta}(w_A\cos\theta - w_y)\right)^2 + \left(\frac{w_y N_c}{2\pi D\cos\theta} - 1\right)^2 & if\ w_A < \frac{\pi D}{N_c} \\ 1 - \frac{1}{8}\left(3 - \frac{N_c}{\pi D}\left(\frac{w_y}{2\cos\theta} + w_A\right)\right)^2 & if\ w_A \geq \frac{\pi D}{N_c} \end{cases} \tag{5}$$

a piecewise function since the open area of the unit cell changes shape depending on w_A.

2.3. Special Case Regular Triaxial Braid

In a maypole braider, the effective number of horngears can be reduced by using fewer carriers, grouping the remaining horngears into functional groups. For example:

- A 12-horngear braider with 8 carriers (4 in each direction) can produce an 8-yarn regular braid with 4 crossover regions.
- This setup functionally divides the 12 horngears into 4 groups of 3 gears each.
- Axial yarns can be inserted through the centre of all horngears in these groups, alternating with the biaxial (braided) yarns in an inverse pattern.

Figure 3 shows this with (a) demonstrating the placement of a typical axial yarn, going under the grey yarns and over the black ones relative to the reader, and Figure 3 (b) demonstrates the special case where the axial yarn is the inverse, going under the black yarns and over the grey yarns.

Similar to the other cases, the dimensions of this axial yarn can be found geometrically knowing that half the unit cell must be greater than two unit cell crossover regions:

$$\frac{\pi D}{N_c} > \frac{w_y}{\cos\theta} \tag{6}$$

If this holds true, then the space for the axial yarn is (Figure 3 (b))

$$\frac{\pi D}{N_c} - \frac{w_y}{\cos\theta} \geq w_A \tag{7}$$

which is the difference between half the unit cell and the crossover regions. Equation (7) can then be rearranged to find the minimum diameter for the special case triaxial braid as

$$D_{min} = \frac{N_c}{\pi}\left(w_A + \frac{w_y}{\cos\theta}\right) \tag{8}$$

the equation for the CF for the special case of triaxial braid will be developed in future studies.

2.4. Diamond Triaxial Braid

Figure 3 (c) shows that the axial yarn width for a diamond braid is the space in the open region between crossover regions. Therefore, we can pose that,

$$w_o \geq w_A \tag{9}$$

w_o is defined as

$$w_o = \frac{2\pi D}{N_c} - \frac{w_y}{\cos\theta} \tag{10}$$

By replacing the equality of equation (9) in equation (10), we obtain the triaxial diamond braid minimum diameter, as,

$$D_{min} = \frac{N_c}{2\pi}\left(\frac{w_y}{\cos\theta} + w_A\right) \tag{11}$$

Therefore, the addition of an axial yarn in a diamond braid will increase the minimum diameter of the mandrel as a function of w_A. The CF for a triaxial diamond braid can be found as,

$$CF_{3ax,dia} = 1 - \left(1 - \frac{w_y N_c}{4\pi R\cos\theta} - \frac{w_A N_c}{4\pi R}\right)^2 = 1 - \left(1 - \frac{N_c\left(w_y + w_A\cos\theta\right)}{4\pi R\cos\theta}\right)^2 \tag{12}$$

where the cover factor is defined as one minus the ratio of open surface area in the unit cell to total surface area. Finding the new area of the open region in the unit cell as a function of the added axial yarn, w_A and finding the ratio gives the contribution of the axial yarn in the $CF_{3ax,dia}$.

3. Experimental Materials and Methods

3.1. Materials

CF/Polyetherketoneketone (PEKK) pre-impregnated composite tapes (APC, AS4D 12K, Syensqo) are used in this work [16]. The data sheet from the manufacturer states a thickness of 0.140 mm resin volume fraction of 34%. The unconsolidated tapes had a thickness of 0.220 ± 0.008 mm, a fibre volume fraction of 64 ± 7 %, and a void volume fraction of 16 ± 3 % [17].

3.2. Maypole Braider

A 12-horngear maypole braider (KBL-24-1-110, Xuzhou Henghui Braiding Machine Co., Ltd.) fabricated the braids. Flexible tubing of 25.4 mm, 34.9 mm, and 60.3 mm diameters served as the mandrels. The mandrel-driving wheel operated too slowly to prevent the braid from braiding over itself, so horngear rotation and mandrel pulling were performed manually. Through holes of with a diameter of approx. 6.4 mm in the horngears allowed the addition of axial yarns for triaxial braids. The maypole braider carriers were adjusted to accommodate the prepreg tapes, with care taken to avoid excessive folds and turns that could damage the yarns. Enclosed yarn guides and a one-way ratchet system prevented the tape from unwinding.

3.3. Yarn Slitting

The initial prepreg tape, a 12-inch continuous sheet, required slitting into smaller strips for usability. An in-house slitting system produced 12.7 mm and 6.4 mm slit tapes, called yarns in this study. The system uses a motor driving two oppositely spinning bobbins. A roller repeatedly slits the 304.8 mm tape in half to obtain a 76.2 mm strip for 12.7 mm yarns or a 38.1 mm strip for 6.4 mm yarns. Razor blades then cut the penultimate strip into six parts to achieve the final yarn width. This process is repeated as needed to produce the required number of yarns.

3.4. Braid Fabrication

Table 1. Experimental layout for preliminary tests, all samples used braiding yarns 12.7 mm wide.

Braid Name	Type	w_A (mm)	Target θ (deg)	Target D (mm)	D_{min} (mm)	Nominal CF (%)
DB-35	Diamond Biaxial	None	45	34.9	34.3	100.0
DB-51	Diamond Biaxial	None	45	50.8	34.3	89.5
DT-35	Diamond Triaxial	6.4	45	34.9	46.5	100.0
DT-60	Diamond Triaxial	6.4	45	60.3	46.5	94.7
RB-25	Regular Biaxial	None	45	25.4	22.9	99.0
RTS-35	Regular Triaxial Special	6.4	45	34.9	62.0	-

Table 1 shows a summary of the tested factors. All braids were done with a w_y of 12.7 mm. The braids are named with an acronym composed of the braid type followed by the target diameter rounded to the unit. The braid types were DB for biaxal diamond, DT for triaxial diamond, RB for biaxial regular, and RTS for the special case of regular triaxial braid (see Section 2.3). For triaxial braids, the w_A was 6.4 mm. The target θ was 45° for all braids. Braids were constructed using flexible mandrels of 25.4 mm, 34.9 mm and 60.3 mm. The braids D_{min} and nominal CF were calculated. For braids DT-35 and RTS-35, the mandrel was smaller than D_{min} to test and verify if the prepreg tapes hold their shape and whether the result agrees with the minimum diameter calculated. After braiding, the pre-forms were soldered on a steel tube smaller than or equal to the actual braid diameter as a curved substrate to support the soldering. Diamond and regular braids were constructed with 12 carriers and 8 carriers respectively. With both types having 12 axial yarns through them when made into a triaxial braid. Image analysis with Gimp and the fiji package of imageJ were used to find θ and the CFs of the fabricated braids.

4. Experimental Results and Discussion

Figure 4 shows the braids fabricated according to the nominal parameters of Table 1. Table 2 lists the measurements made on the braids of Figure 4. For most of the braids, the measured θ was lower than the target value of 45°. Braid angle control proved challenging with the current setup. Prepreg tapes followed a standard "path of least resistance" around the mandrel, aligning flush and minimizing scaling effects such as undesired yarn twist. Upon mandrel removal, biaxial braids DB-35, DB-51 and RB-25 straightened, reducing both θ and D until reaching a low-angle jammed state. The biaxial braids were placed on steel mandrels having their respective targeted diameter and stabilized by soldering the ends to retain braid structure without jamming. Therefore, the measured D of DB-35, DB-51 and RB-25 are close to the targeted values.

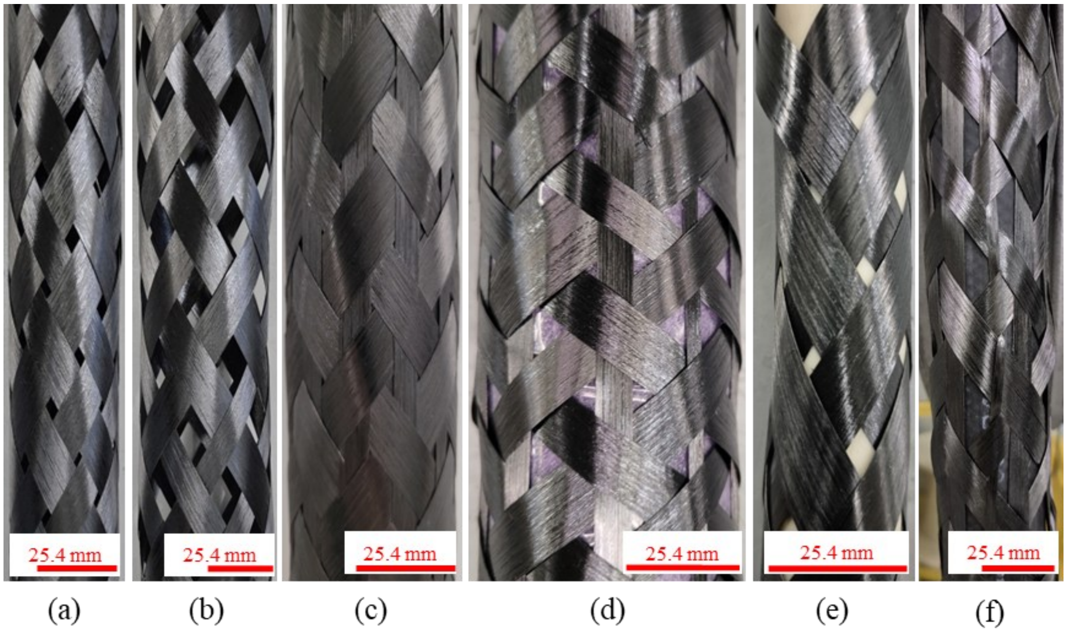

Figure 4. Images of fabricated braids (a) DB-35, (b) DB-51, (c) DT-35, (d) DT-60, (e) RB-25, (f) RTS-35,

Table 2. Table of constructed braids and their measured braid angles and cover factors

Braid Name	Measured θ (deg)	Difference θ	Measured D (mm)	Adjusted D_{min} (mm)	Adjusted Nominal CF (%)	Measured CF (%)	Difference with Nominal CF
DB-35	27.6±0.6	-17.4	34.9	27.4	98.1	97.5	0.6
DB-51	30.3±0.6	-14.7	50.8	28.2	80.1	79.9	0.2
DT-35	37.2±0.6	-7.8	44.5	42.7	99.8	98.9	0.9
DT-60	49.5±0.8	+4.5	60.3	49.5	96.7	95.9	0.8
RB-25	36.2±1.7	-8.8	25.4	20.1	95.6	91.2	4.4
RTS-35	37.6±2.3	-7.4	41.9	56.9	-	80.9	-

The triaxial braids kept their structure after braiding since the axial yarns stabilized the structure. Braiding of DT-60 had a measured θ and D closer to the targeted values. This is explained by the fact that the mandrel diameter was large. The stiff prepreg tapes could bend around the mandrel with more ease. For DT-35 and RTS-35, braiding on mandrels slightly smaller than the D_{min} (see Table 1) produced jammed structures that did not deposit onto the mandrel. However, the measured Ds are not equal to the D_{min}s of Table 1 since the measured θ are different from the target.

Table 2 shows adjusted D_{min} and adjusted nominal CF values that were calculated to account for the significant changes in θ. The measured CF results in Table 2 are similar to the adjusted nominal CF values with errors below 5%. This demonstrates strong agreement between measured and calculated values. The variations may be due to slightly variable axial or biaxial yarn widths.

5. Conclusion

This study examines the relationship between mandrel diameter and braid/axial yarn widths in TBCs with prepreg tape yarns. Prepreg yarns, feature a rigid cross-section, conforming less to the mandrel's tubular shape during braiding. The minimum D, maximum w_A and corresponding CF were determined for biaxial and triaxial diamond and regular braids. Additionally, a special case triaxial regular braid with an inverse middle axial yarn was analyzed. Preliminary CF/PEKK braids were then fabricated with and without axial yarns, varying braid type and D to validate the predicted geometry in TBC prepreg braiding. Controlling θ proved difficult with the current setup, as the rigidity of the tape yarns caused them to straighten into specific helical paths around the mandrel. However, the specific geometry of a braid for a given θ was easier to predict and design due to the consistent yarn cross-section size and shape. Future work will focus on improving the tape carriers, enhancing position control and tension regulation, and using a larger braider with better speed control to achieve the targeted braid angle.

6. References

1. Canada, T. *Advanced air mobility*. 2025 [cited 2025; Available from: https://tc.canada.ca/en/aviation/advanced-air-mobility.
2. Kaw, A.K., *Mechanics of Composite Materials*. Second ed. Mechanical Engineering Series, ed. F. Kreith. 2006: CRC Press Taylor & Francis Group.
3. Lee, J.S. and J.W. Kim, *Impact Response of Carbon Fibre Fabric/Thermoset-Thermoplastic Combined Polymer Composites.* Advanced Composites Letters, 2017. **26**(3): p. 82-88.
4. Bernatas, R., et al., *Recycling of fibre reinforced composites with a focus on thermoplastic composites.* Cleaner Engineering and Technology, 2021. **5**.
5. Karahan, M., et al., *Comparative study of virgin and recycled polyethylene terephthalate and polypropylene intermingled thermoplastic composites.* Polymer Composites, 2025. **46**(4): p. 3820-3836.
6. Aravinthan Arumugam and A. Pramanik, *A Review on the Recent Trends in Forming Composite Joints Using Spot Welding Variants.* Journal of Composite Science, 2024. **8**(155).
7. Li, H., et al., *Ultrasonic welding of fibre-reinforced thermoplastic composites: a review.* The International Journal of Advanced Manufacturing Technology, 2022. **120**: p. 29-57.
8. El-Jakl, M. and L. Laberge Lebel, *Braid-trusion of hollow thermoplastic composites using an expanding mandrel approach.* Composites Part B, 2025. **305**(112677): p. 10.
9. Mischorr, E., et al., *Advanced manufacturing of thermoplastic tape preforms: braiding simulation, curved preforming, and consolidation via rotational and bladder-assisted molding.* Advanced Manufacturing: Polymer & Composites Science, 2025. **11**(1, 2546292).
10. Carey, J.P., *Handboook of Advances in Braided Composite Materials*. First ed. Woodhead Publishing Series in Composites Science and Engineering. 2017: Woodhead Publishing. 479.
11. Melenka, G.W., et al., *Micro-computed tomography analysis of tubular braided composites.* Composite Structures, 2015. **131**: p. 384-396.
12. Garthaus, C., *Zur Herstellung funktionalisierter Hohlprofilstrukturen aus endlosfaserverstärkten Thermoplasten*, in *Mechanical Engineering*. 2017, Technical University of Dresden: Hannover.
13. Würfel, V., et al., *Inside Hybridization of CF/PAEK Hollow Profiles by Means of Injection Molding.* SAMPE Journal, 2025: p. 12-19.
14. Li, Y., et al., *Manufacturing and Joining of Composite Units for On-Orbit Construction of Large Structures in Space.* Space: Science and Technology, 2026. **6**.
15. Potluri, P., et al., *Geometrical modelling and control of a triaxial braiding machine for producing 3D preforms.* Composites Part A, 2003. **34**: p. 481-492.
16. Solvay, *Technical Data Sheet APC (PEKK-FC)*, in *PEKK-FC Thermoplastic Polymer Prepreg*. 2017, Solvay: Alpharetta, GA, USA.
17. Hamon, E. and L. Laberge Lebel, *Multi-die thermoplastic pultrusion of carbon reinforced PolyEtherKetoneKetone bars at 1 m/min using preimpregnated tape.* Composites Part B, 2026. **312**.